# *Electronic Supplementary Information*

# Porous Zn-MOF with two diverse cages synthesized using functionalized biphenyl tricarboxylic acid: $CO_2$ selective adsorption and fixation

Nan An,[a] Lu-Lu Ma,[a] Fan Yang,[a] Wen-Yan Zhang, [a] Guo-Ping Yang,*[a] and Yao-Yu Wang*[a]

[a]*Key Laboratory of Synthetic and Natural Functional Molecule of the Ministry of Education, Shaanxi Key Laboratory of Physico-Inorganic Chemistry, Xi'an Key Laboratory of Functional Supramolecular Structure and Materials, College of Chemistry & Materials Science, Northwest University, Xi'an 710127, Shaanxi, P. R. China.*

*E-mail: ygp@nwu.edu.cn; wyaoyu@nwu.edu.cn*

**Materials and general methods.**

The powder X-ray diffraction (PXRD) data were tested on Bruker D8 ADVANCE X-ray powder diffractometer. Thermogravimetric analyses (TGA) were performed on the NETZSCH STA 449C microanalyzer thermal analyzer under a $N_2$ atmosphere. The infrared spectra (IR) data were tested in the range of 400-4000 cm$^{-1}$ on Bruker Equinox-55 FT-IR spectrometer. Gas sorption isotherms were performed on an ASAP 2020 M sorption equipment using 30mg of MOFs. $^1$H NMR spectrograms were gained on a Bruker Ascend 400 (400 MHz) spectrometer.

**Table S1.** Selected bond lengths (Å) and bond angles (°) for **1**.

| Complex 1 | | | |
|---|---|---|---|
| Zn(1)-Zn(1)#1 | 2.778(4) | O(2)#6-Zn(2)-O(7)#7 | 102.4(6) |
| Zn(1)-O(1) | 1.982(9) | O(3)-Zn(2)-Zn(2)#5 | 122.4(5) |
| Zn(1)-O(1)#2 | 1.982(9) | O(3)-Zn(2)-Zn(2)#4 | 122.6(4) |
| Zn(1)-O(4)#1 | 1.992(9) | O(3)-Zn(2)-O(5) | 107.5(7) |
| Zn(1)-O(4)#3 | 1.992(9) | O(3)-Zn(2)-O(7)#7 | 116.8(7) |
| Zn(1)-O(6) | 2.083(12) | O(5)-Zn(2)-Zn(2)#4 | 36.0(2) |
| Zn(2)-Zn(2)#4 | 3.132(3) | O(5)-Zn(2)-Zn(2)#5 | 36.0(2) |
| Zn(2)-Zn(2)#5 | 3.132(4) | O(7)#7-Zn(2)-Zn(2)#5 | 118.3(5) |
| Zn(2)-O(2)#6 | 1.903(11) | O(7)#7-Zn(2)-Zn(2)#4 | 75.1(4) |
| Zn(2)-O(3) | 1.921(13) | O(7)#7-Zn(2)-O5 | 110.8(5) |
| Zn(2)-O(5) | 1.935(6) | O(3A)#5-Zn(2A)-O(5) | 97(3) |
| Zn(2)-O(7)#7 | 1.931(13) | O(3A)#5-Zn(2A)-O(7A)#8 | 140(4) |
| Zn(2A)-O(3A)#5 | 1.98(9) | O(5)-Zn(2A)-O(7A)#8 | 95(3) |
| Zn(2A)-O(5) | 2.00(3) | O(8)-Zn(3)-O(5) | 112.1(4) |
| Zn(2A)-O(7A)#8 | 2.37(10) | O(8)#5-Zn(3)-O(5) | 112.1(4) |
| Zn(3)-O(5) | 1.957(17) | O(8)#4-Zn(3)-O(5) | 112.1(4) |
| Zn(3)-O(8)4# | 1.940(10) | O(8)#4-Zn(3)-O(8) | 106.7(5) |
| Zn(3)-O(8)5# | 1.940(10) | O(8)#4-Zn(3)-O(8)5 | 106.7(4) |
| Zn(3)-O(8) | 1.940(10) | O(8)#5-Zn(3)-O(8) | 106.7(5) |
| Zn(3A)-O(2A)#6 | 2.01(10) | O(2A)#8-Zn(3A)-O(2A)#7 | 116.5(19) |
| Zn(3A)-O(2A)#8 | 2.01(10) | O(2A)#6-Zn(3A)-O(2A)#8 | 116.5(19) |
| Zn(3A)-O(2A)#7 | 2.01(10) | O(2A)#6-Zn(3A)-O(2A)#7 | 116.5(19) |
| Zn(3A)-O(5) | 1.94(4) | O(5)-Zn(3A)-O(2A)#8 | 101(3) |
| O(1)-C(4) | 1.221(18) | O(5)-Zn(3A)-O(2A)#7 | 101(3) |
| O(2)-C(10) | 1.256(19) | O(5)-Zn(3A)-O(2A)#6 | 101(3) |
| O(2A)-C(10) | 1.46(11) | C(4)-O(1)-Zn(1) | 122.1(8) |
| O(3)-C(14) | 1.20(2) | C(10)-O(2)-Zn(2)#9 | 127.2(10) |
| O(3A)-C(14A) | 1.21(3) | C(10)-O(2A)-Zn(3A)#10 | 107(5) |
| O(4)-C(4) | 1.219(17) | C(14)-O(3)-Zn(2) | 135.5(13) |

| O(7)-C(10) | 1.253(18) | C(4)-O(4)-Zn(1)#2 | 125.7(9) |
| O(7A)-C(10) | 1.61(10) | Zn(2)-O(5)-Zn(2)#5 | 108.1(5) |
| O(8)-C(14) | 1.28(2) | Zn(2)#4-O(5)-Zn(2)#5 | 108.1(5) |
| O(8A)-C(14A) | 1.20(3) | Zn(2)-O(5)-Zn(2)#4 | 108.1(5) |
| O(1)#1-Zn(1)-Zn(1)#2 | 83.2(3) | Zn(2)-O(5)-Zn(2A)#5 | 69.5(9) |
| O(1)-Zn(1)-Zn(1)#2 | 83.2(3) | Zn(2)#5-O(5)-Zn(2A)#5 | 177.4(9) |
| O(1)#1-Zn(1)-O(1) | 166.5(6) | Zn(2)#4-O(5-)Zn(2A)#5 | 73.8(10) |
| O(1)-Zn(1)-O(4)#3 | 89.0(4) | Zn(2)#4-O(5)-Zn(2A)#4 | 177.4(9) |
| O(1)#1-Zn(1)-O(4)#2 | 89.0(4) | Zn(2)-O(5)-Zn(2A)#4 | 73.8(10) |

Symmetry transformations used to generate equivalent atoms: #1 +x, 1-y, -z; #2 1-x, 1-y, +z; #3 1-x, +y, -z; #4 1-x, +y, 1-z,; #5 +x, 1-y, 1-z; #6 1/2-x, 3/2-y, 1/2+z; #7 1/2+x, -1/2+y, 1/2+z; #8 1/2+x, 3/2-y, 1/2-z; #9 3/2-x, -1/2+y, 1/2-z; #10 -1/2+x, 3/2-y, 1/2-z; #11 -1/2+x, -1/2+y, 1/2+z.
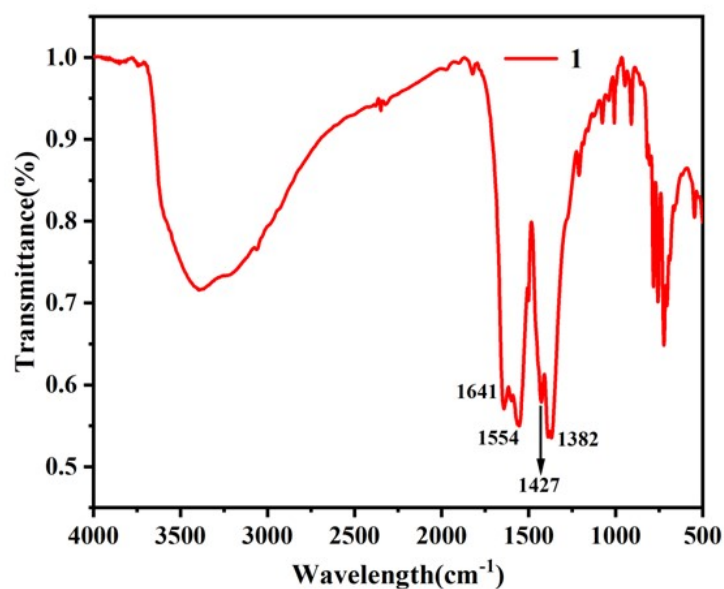


**Fig. S1** The FT-IR spectra of **1** (1641=carbon carbon double bond, 1554=benzene ring, 1427, 1382=hydrocarbon bond).
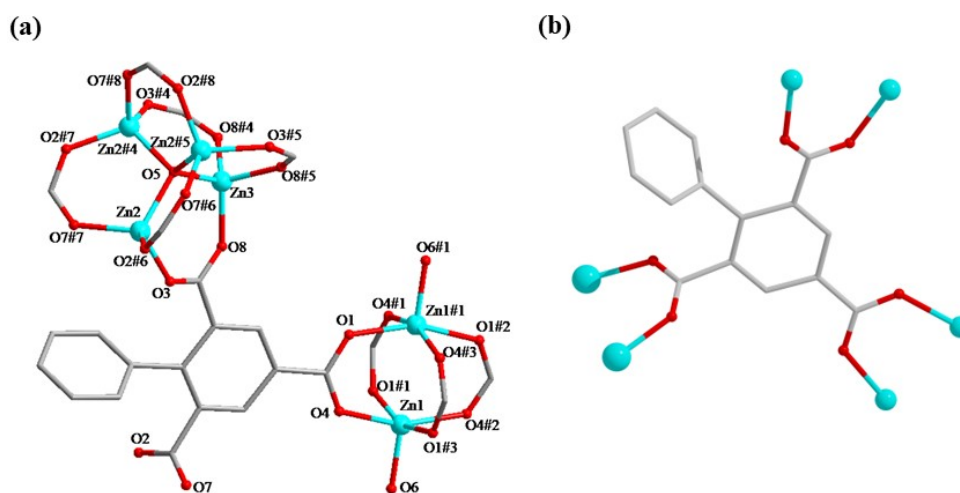


**Fig. S2** (a) Coordination environment diagram of **1**. (b) The coordination modes of L$^{3-}$ in **1**.
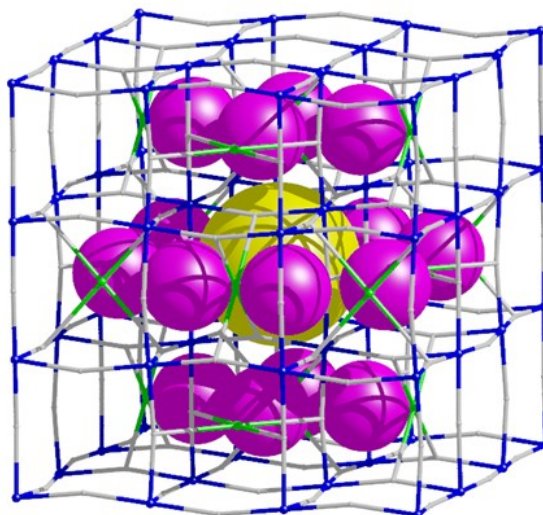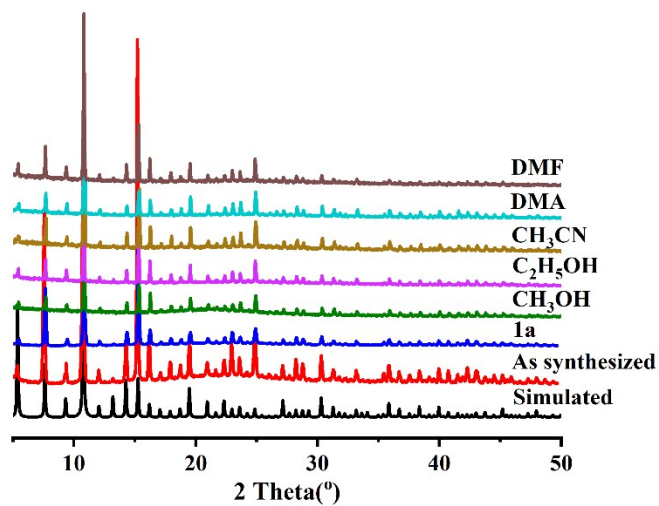
**Fig. S3** The topological net for **1**.



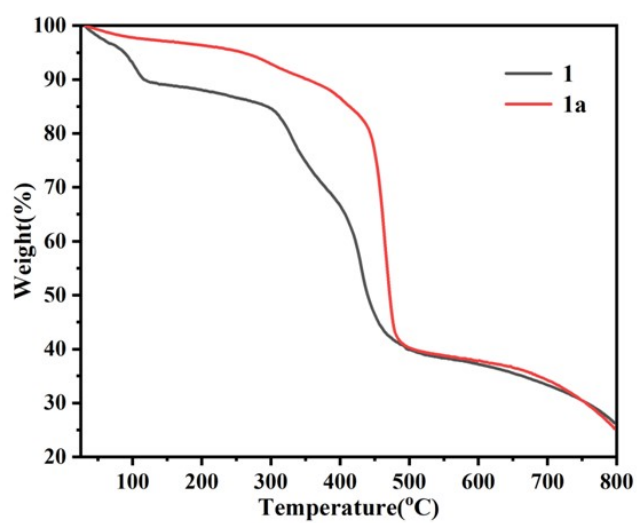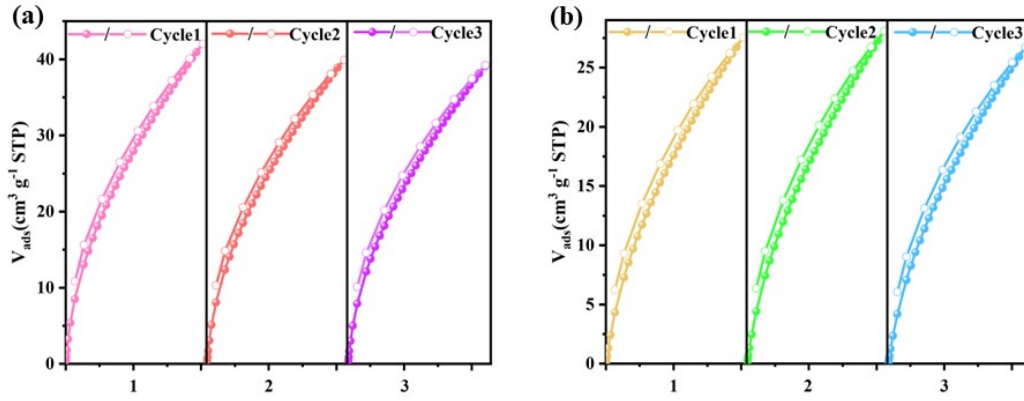**Fig. S4** PXRD patterns of **1**, **1a** and **1** at different common solvents (.



**Fig. S5** The TGA plots of **1** and **1a** under $N_2$ environment.

**Fig. S6** $CO_2$ reabsorption experiments at different temperatures: 273 K (a) and 298 K (b)

**Calculation of sorption heat for gas using Virial 2 model**

$$\ln P = \ln N + 1/T\sum_{i=0}^{m}a_iN^i + \sum_{i=0}^{n}b_iN^i$$

$$Q_{st} = -R\sum_{i=0}^{m}a_iN^i$$

Above virial expression was used to fit the combined isotherm data for 1a at 273.15 and 298 K, where $P$ is the pressure, $N$ is the adsorbed amount, $T$ is the temperature, $a_i$ and $b_i$ are virial coefficients, and $m$ and $N$ are the number of coefficients used to describe the isotherms. $Q_{st}$ is the coverage-dependent enthalpy of adsorption and $R$ is the universal gas constant.
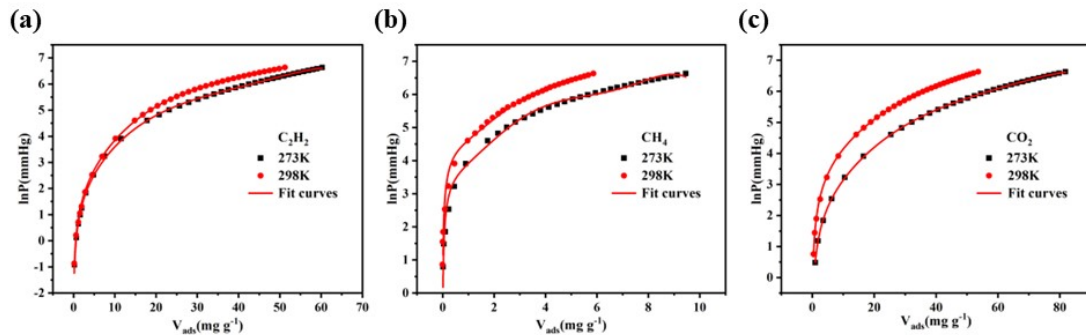


**Fig. S7** (a) $C_2H_2$, a0 = -397.0335, a1 = 40.95674, a2 = -47.48092, a3 = -0.02085, a5 = -4.10052E-6, b0 = 1.92079, b1= 0.26785, b2=-0.00366, Chi^2 = 0.00443, R^2 = 0.99911. (b) $CH_4$, a0 = -2470.79298, a1 = 36.70724, a2 = 187.05099, a3=-58.89557, a4=6.24143, b0 = 13.72709, b1=-1.59287, b2=0.20751, Chi^2 = 0.08251, R^2 = 0.97016. (c) $CO_2$, a0 = -3667.28881, a1 = 41.78032, a2 = -0.03396, a3=-0.01236, a4=1.61371E-4, a5=-7.29678E-7, b0 =13.94246, b1=-0.12791, b2=0.00128, Chi^2 = 3.84946E-4, R^2 = 0.99987.

**Selectivity prediction via IAST**

The experimental isotherm data for pure gas A, and gas B were fitted at 298 K using a dual Langmuir-Freundlich (L-F) model (Figure S7):

$$q = \frac{a_1 * b_1 * p^{c_1}}{1 + b_1 * p^{c_1}} + \frac{a_2 * b_2 * p^{c_2}}{1 + b_2 * p^{c_2}}$$

Where $q$ and $p$ are adsorbed amounts and the pressure of component $i$, respectively.

The adsorption selectivities for binary mixtures of gas A/gas B, defined by

$$S_{i/j} = \frac{x_i * y_j}{x_i/y_j}$$

were respectively calculated using the Ideal Adsorption Solution Theory (IAST) of Myers and Prausnitz. Where $x_i$ is the mole fraction of component $i$ in the adsorbed phase and $y_i$ is the mole fraction of component i in the bulk.
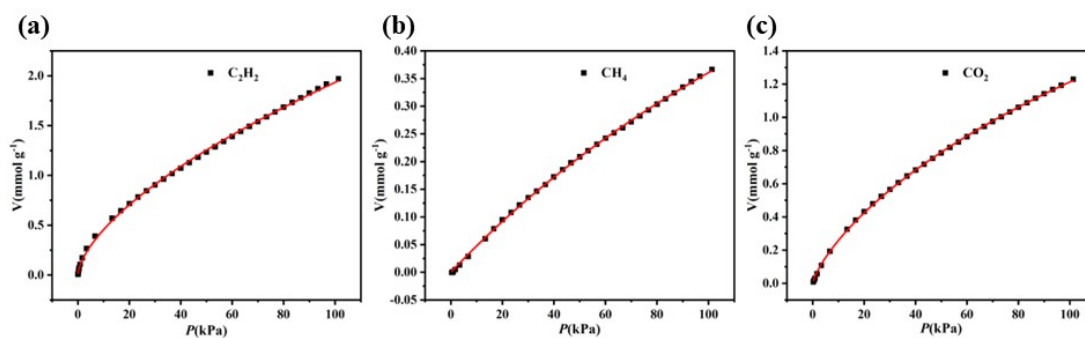


**Fig. S8** (a) $C_2H_2$, a1 = 193.65101, b1 = 5.52032E-4, c1 = 0.63093, Chi^2 = 2.88567E-4, R^2 = 0.99929; (b) $CH_4$, a1 = 1.38534, b1 = 0.0036, c1 = 0.99494, Chi^2 = 4.61392E-6, R^2 = 0. 0.99967; (c) $CO_2$, a1 = 5.21952, b1 = 0.00897, c1 = 0.76415, Chi^2 = 3.44731E-5, R^2 = 0.99976.
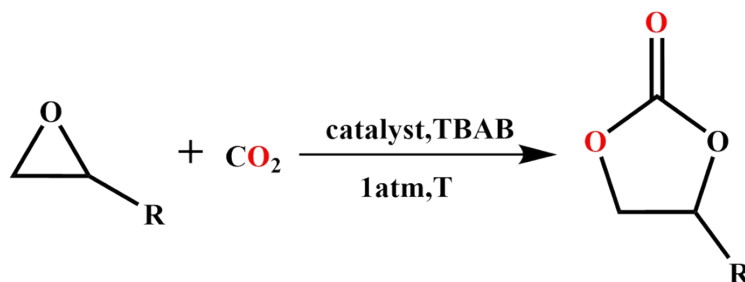


**Scheme S1** $CO_2$ cycloaddition equation.

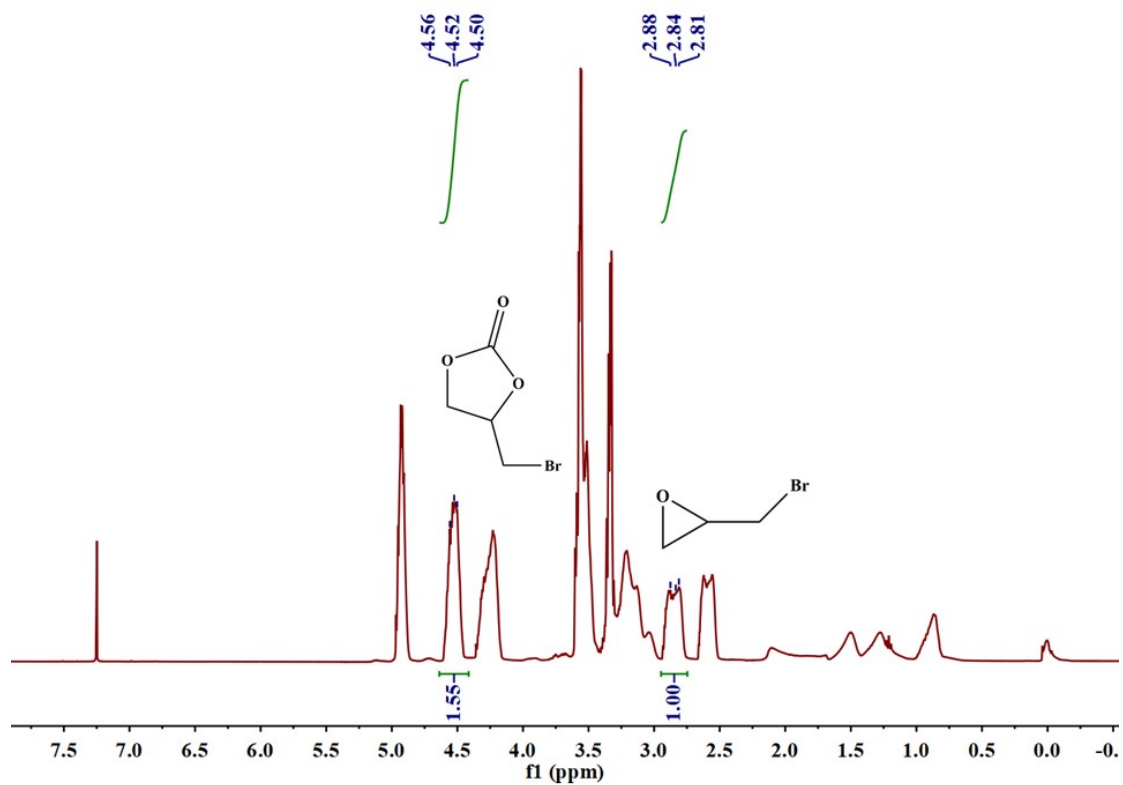**Fig. S9** $^1$H NMR spectrum of 4-bromomethyl -1,3-dioxolan-2-one in CDCl$_3$. (Table 2, entry 1).



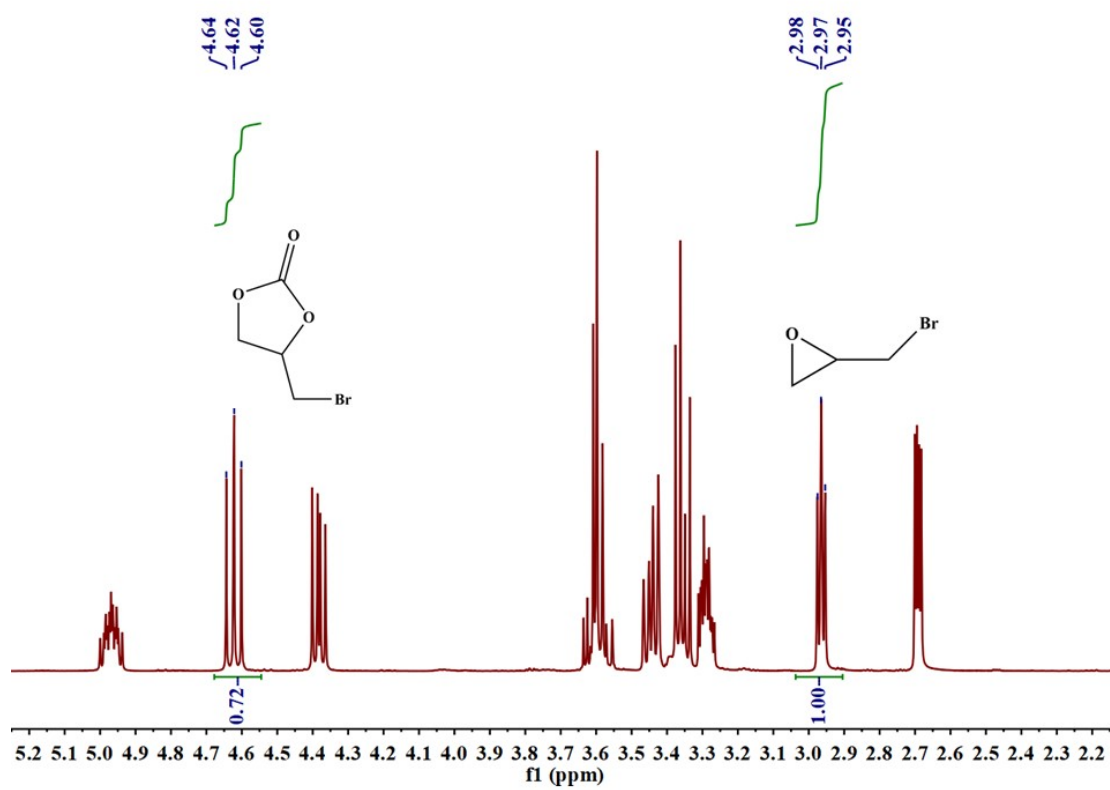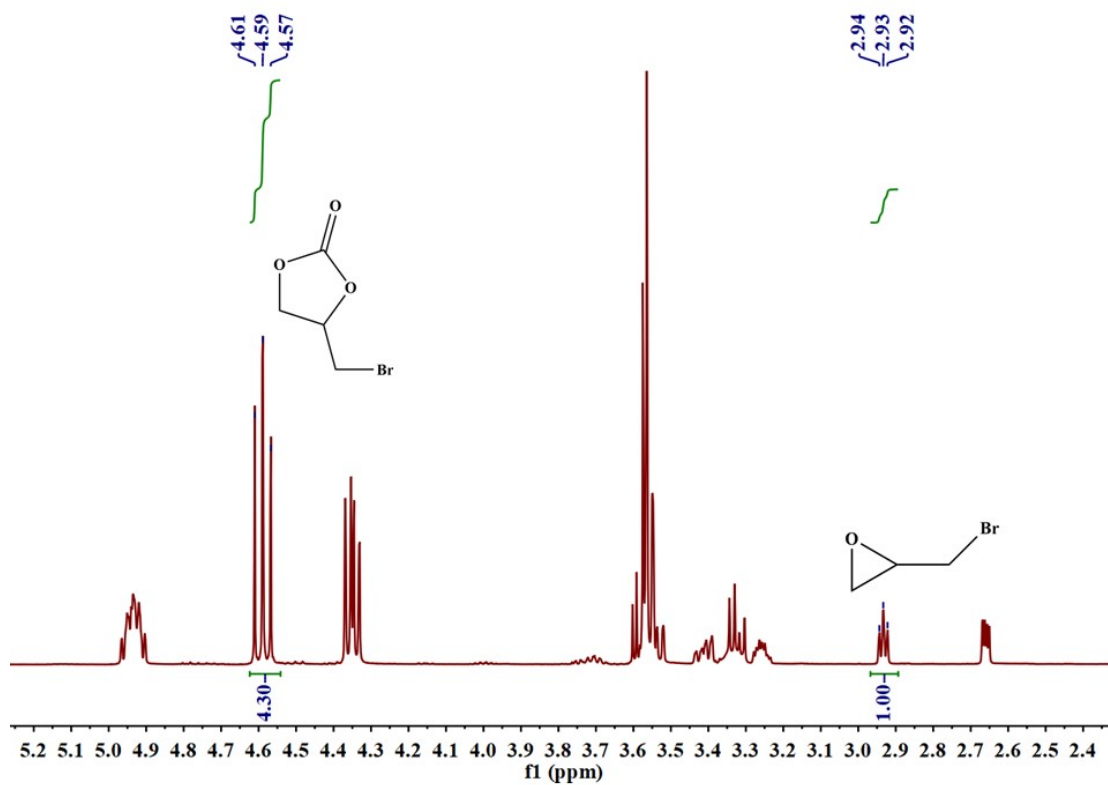**Fig. S10** $^1$H NMR spectrum of 4-bromomethyl -1,3-dioxolan-2-one in CDCl$_3$. (Table 2, entry 2).

**Fig. S11** $^1$H NMR spectrum of 4-bromomethyl -1,3-dioxolan-2-one in CDCl$_3$. (Table 2, entry 3).



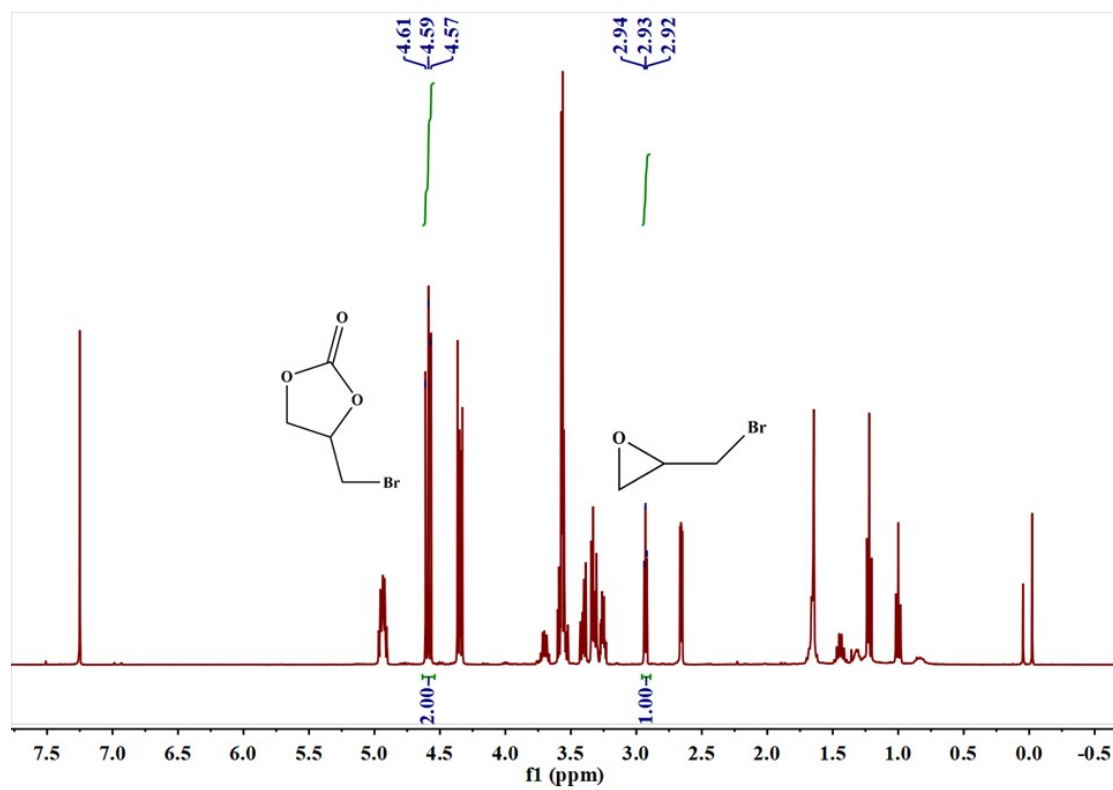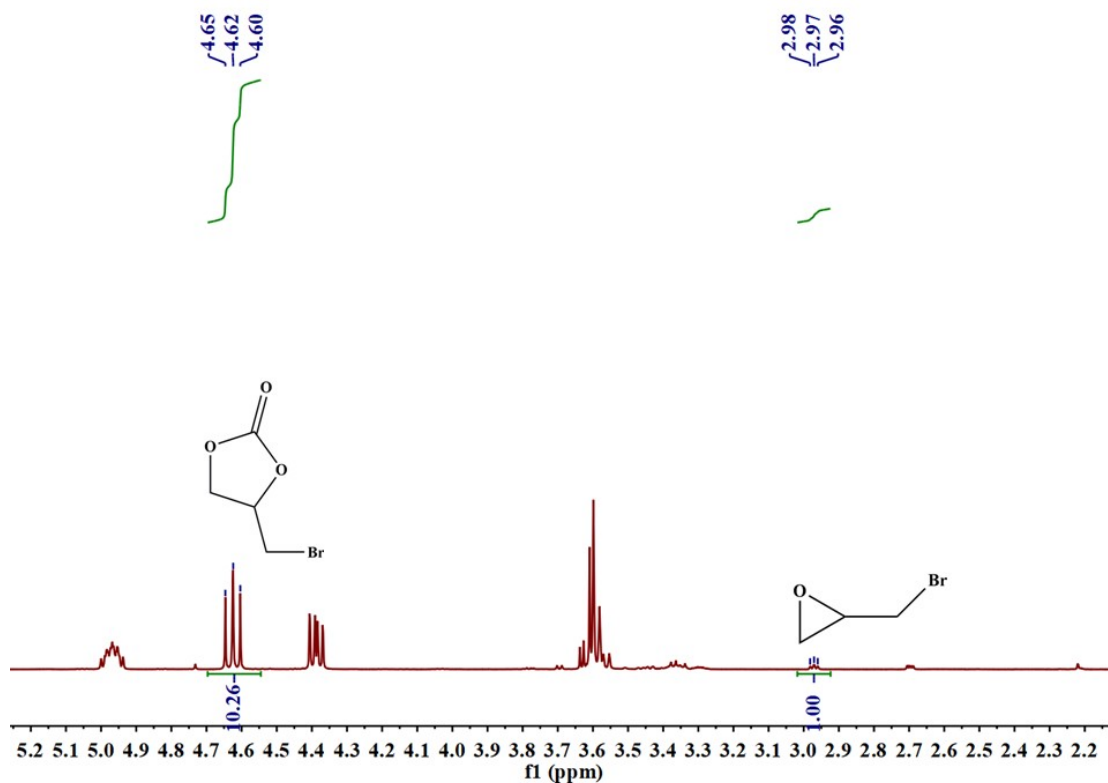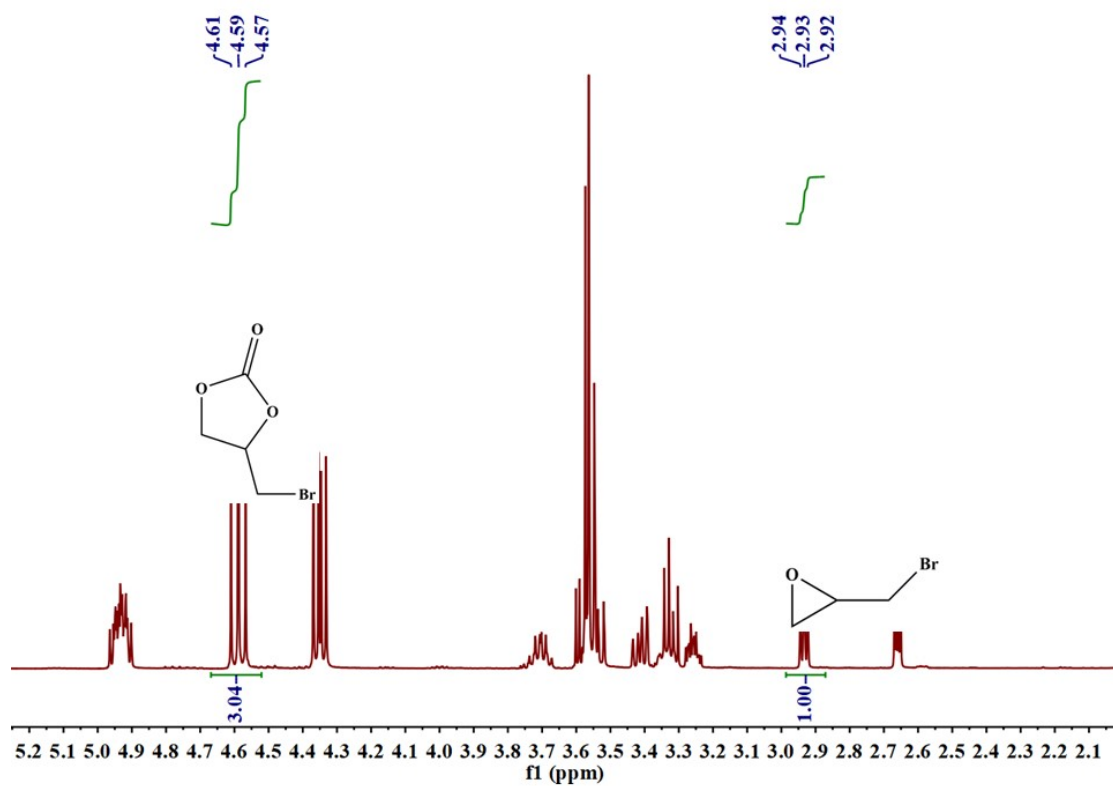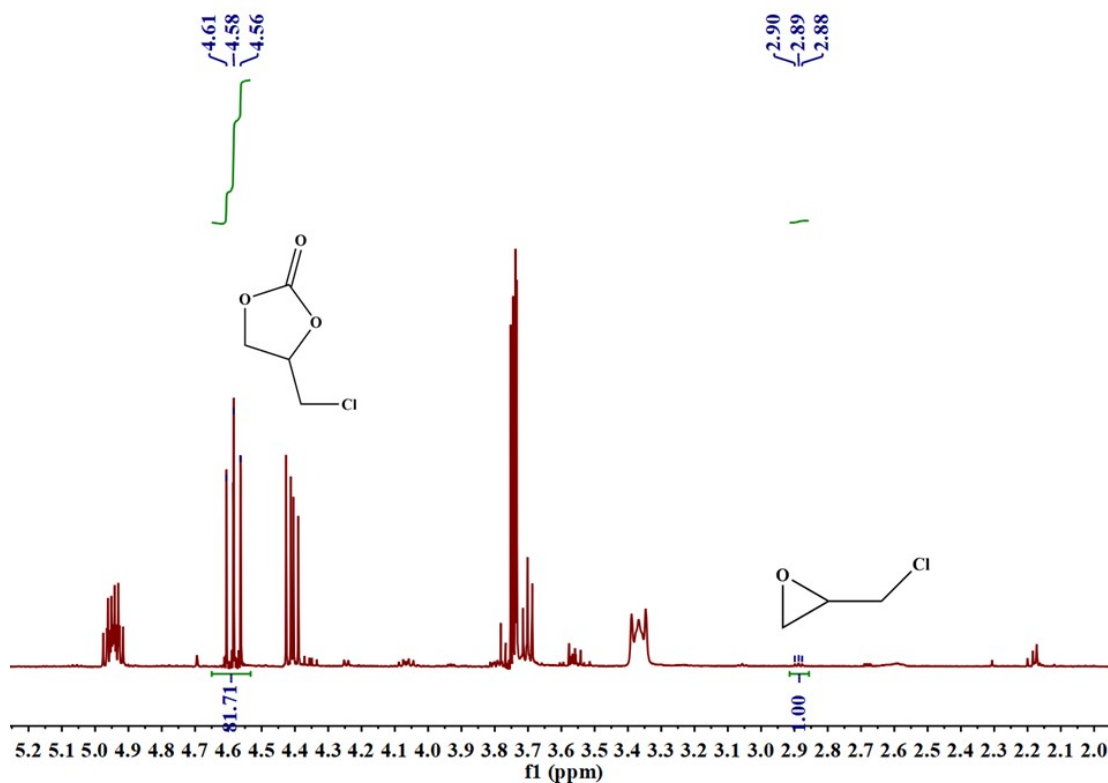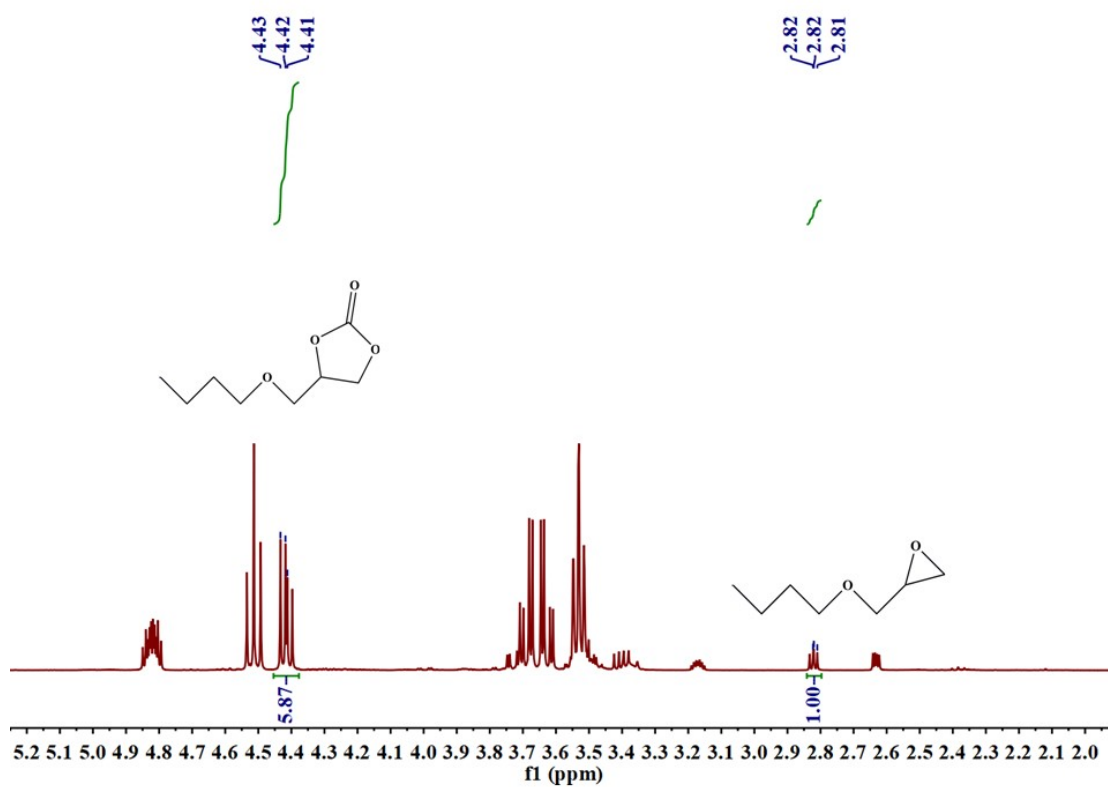**Fig. S12** $^1$H NMR spectrum of 4-bromomethyl -1,3-dioxolan-2-one in CDCl$_3$. (Table 2, entry 4).

**Fig. S13** ^{1}H NMR spectrum of 4-bromomethyl -1,3-dioxolan-2-one in CDCl$_3$. (Table 2, entry 5).



**Fig. S14** ^{1}H NMR spectrum of 4-bromomethyl -1,3-dioxolan-2-one in CDCl$_3$. (Table 2, entry 6).

**Fig. S15** ${}^1$H NMR spectrum of 4-cloromethyl-1,3-dioxolan-2-one in CDCl$_3$. (Table 2, entry 7).



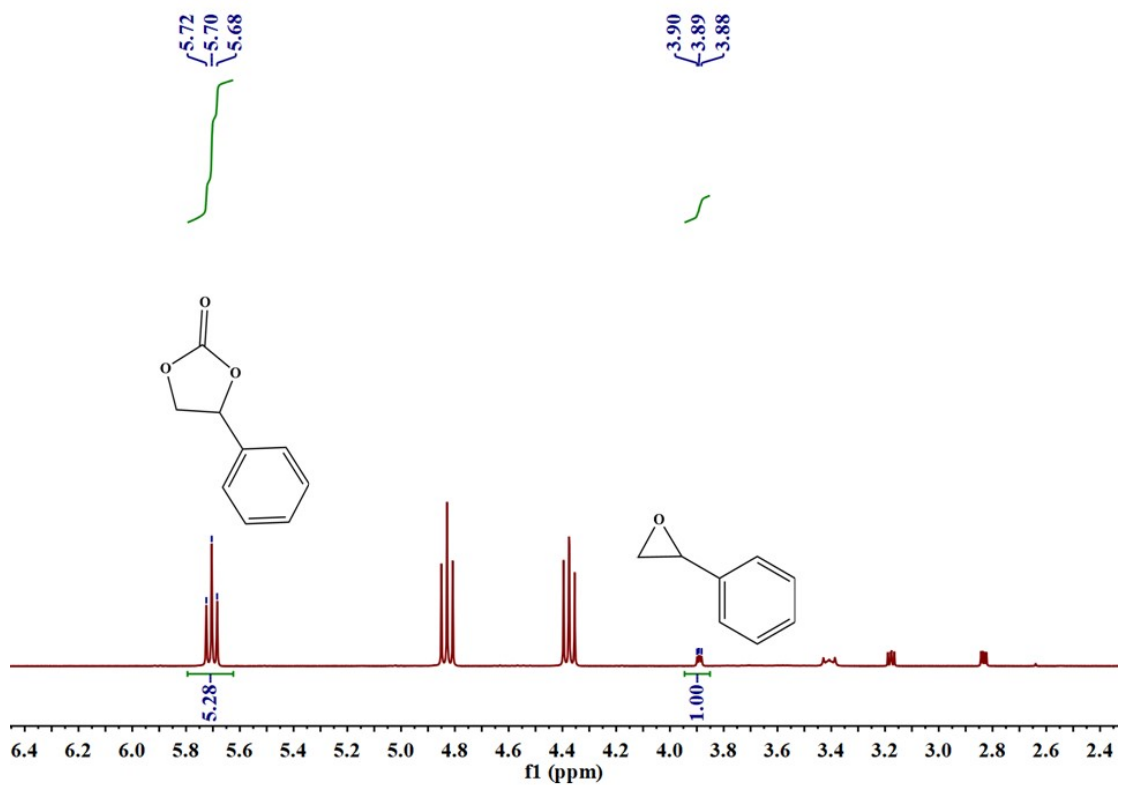**Fig. S16** ${}^1$H NMR spectrum of 3-butoxy-1,2-propylene carbonate in CDCl$_3$. (Table 2, entry 8).

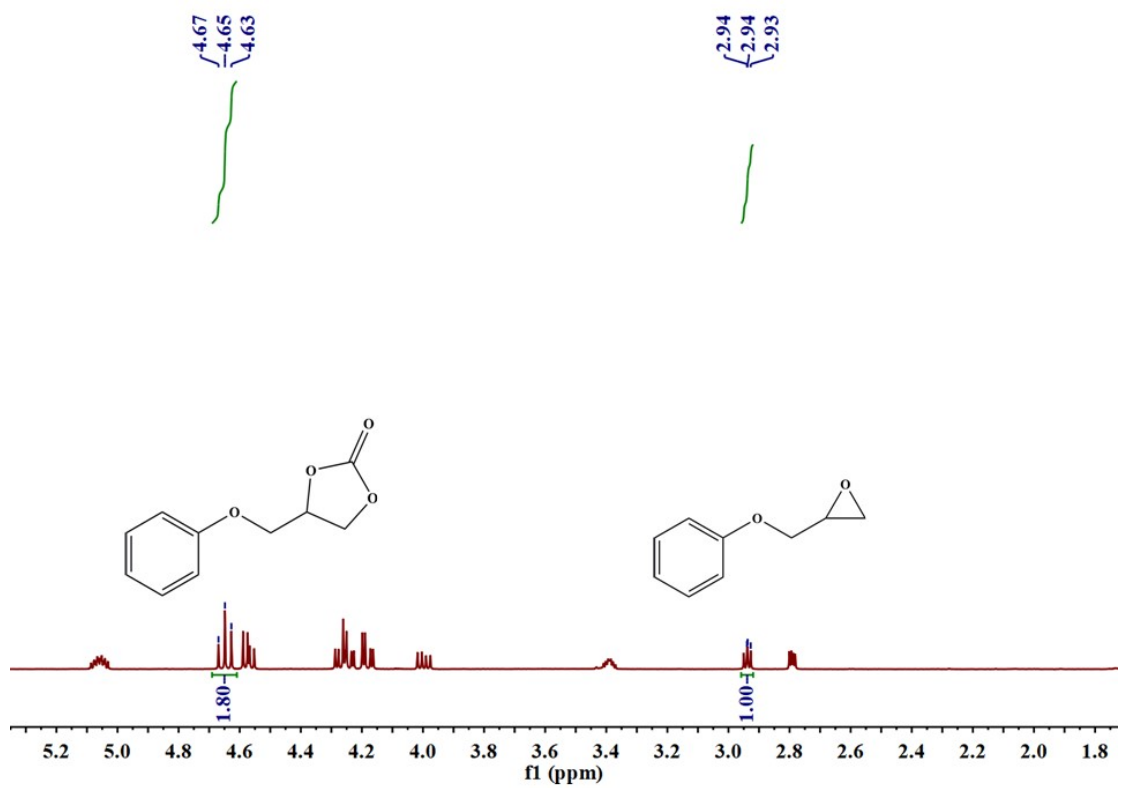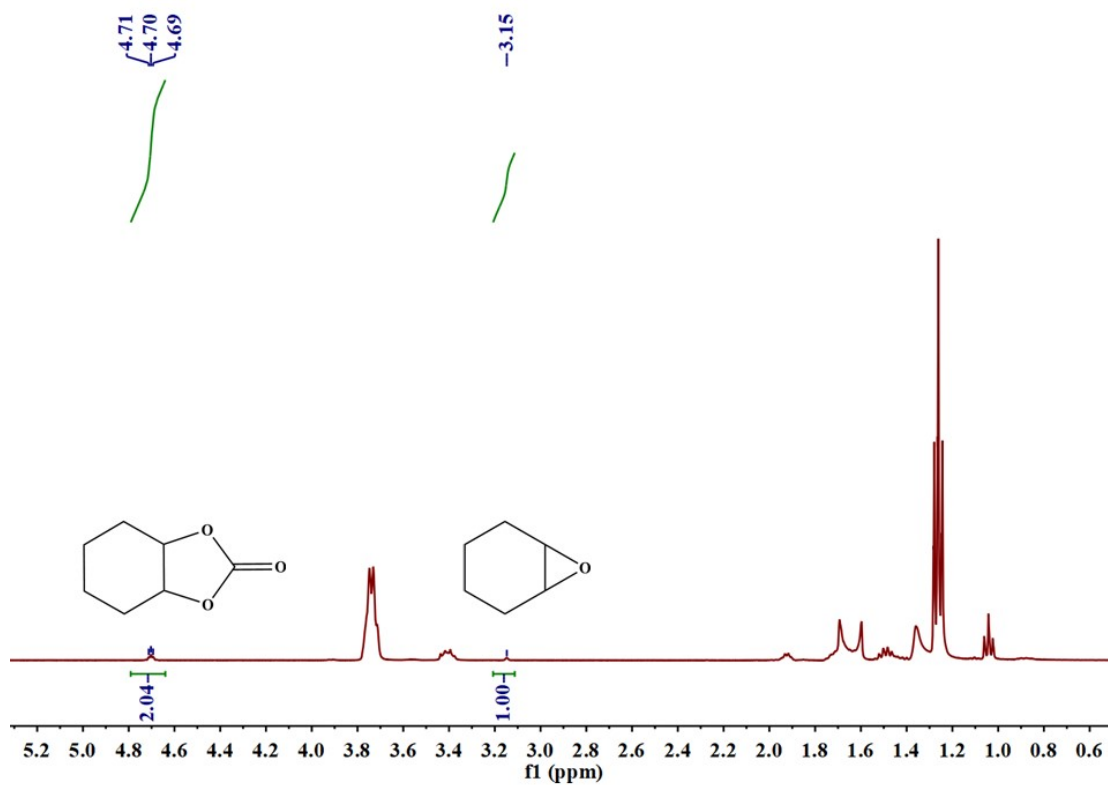**Fig. S17** $^{1}$H NMR spectrum of styrene carbonate in CDCl$_3$. (Table 2, entry 9).



**Fig. S18** $^{1}$H NMR spectrum of 4-(phenoxymethyl)-1,3-dioxolan-2-one in CDCl$_3$. (Table 2, entry 10).

**Fig. S19** ^{1}H NMR spectrum of benzo[1,3]dioxol-2-one with **1**. (The solvent is CDCl$_3$).